ROBOTIC DEPLOYMENT OF EXTRATERRESTRIAL SEISMIC NETWORKS

Daniel Leidner[1], **Selma Musić**[2], **and Armin Wedler**[1]

[1]*German Aerospace Center (DLR), Institute of Robotics and Mechatronics, Germany, 82234 Weßling, daniel.leidner@dlr.de, armin.wedler@dlr.de*

[2]*Technische Universität München (TUM), Institute for Information-Oriented Control, Germany, 80333 München, music@lsr.ei.tum.de*

ABSTRACT

Manual installation of seismic networks in extraterrestrial environments is risky, expensive and error-prone. A more reliable alternative is the automated deposition with a light-weight robot manipulator. However, inserting a spiked sensor into soil is a challenging task for a robot since the soil parameters are variable and difficult to estimate. Therefore, we investigate an approach to accurate insertion and positioning of geophones using a Cartesian impedance controller with a feed-forward force term. The feed-forward force component of the controller is either estimated using the Fundamental Earth-Moving Equation, the Discrete Element Method or empirically. For the first time, both the geological aspects of the problem as well as the aspects of robotic control are considered. Based on this consideration, the control approach is enhanced by predicting the resistance force of the soil. Experiments with the humanoid robot Rollin' Justin inserting a geophone into three different soil samples validate the proposed method.

Key words: Robotic Space Exploration, Seismic Networks, Compliant Manipulation, Soil-Tool Interaction.

1. INTRODUCTION

To investigate sub-surface properties and seismic activity of extraterrestrial environments, such as the Moon, seismic networks need to be deployed at the surface onsite. However, the manual installation of extraterrestrial seismic networks, i. e. geophones, is risky, expensive and error-prone. Evidence for this can be found in the reports of the *Active Seismic Experiment (ASE)* conducted during the *Apollo* missions [1]. During the Apollo 14 mission, the astronauts emplaced the so-called *Apollo Lunar Surface Experiments Package (ALSEP)*, which constitutes a seismic network consisting of a seismometer and a string of three spiked geophones. The mission report states that the lunar soil gave little resistance to hold the geophones in place causing them to tilt after inserting them into the ground. The astronauts where forced to repeatedly adjust the sensors to guarantee good coupling with the soil and an upright position with less than seven degree tilt error.

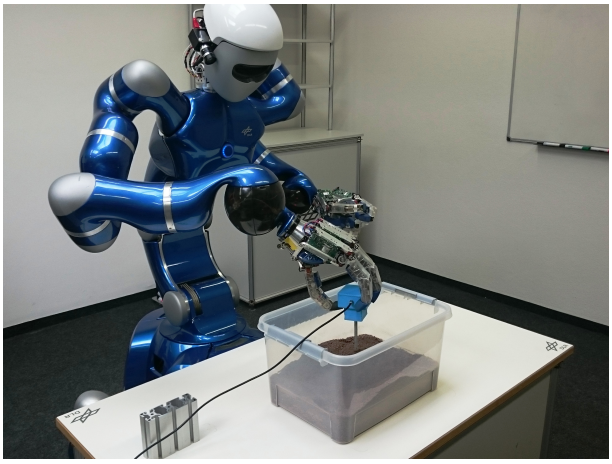

Figure 1. The humanoid robot Rollin' Justin inserting a geophone dummy into Martian soil simulant.

As a consequence the astronauts took longer than planned to setup the experiment. Moreover, The *Lunar Reconnaissance Orbiter (LRO)* recently captured images of additional seismic instruments deployed during the Apollo 17 mission. Czeluschke *et al.* [2] found out that these images show significant differences between previously published and LRO-based source-receiver distances of up to 40 m, resulting in inaccurate assumptions of the lunar sub-surface properties.

A more reliable solution is the automated sensor deposition by a robotic manipulator, allowing for efficient, precise and repeatable task completions. Sensing capabilities to measure force and torque enable a compliant robot to fulfill this task w. r. t. the requirements of the geological experiments. This paper describes the experimental validation of this issue as part of the *ROBEX* project [3]. In a laboratory environment, a suite of experiments is conducted to validate the automated deployment procedure under varying condition. These experiments serve as proof of concept for the upcoming field mission to be held at a planetary analogue site. During this mission, the LRU Rover [4] equipped with a light weight manipulator will deploy an active seismic network which resembles the ALSEP setup deployed during the Apollo missions [1]. The geophones of the seismic network have to be aligned precisely w. r. t. the vertical and lateral directions.

Moreover, specific forces have to be applied to ensure good coupling between the geophone spike and the soil, which is important for the geological measurements.

In this work we propose a control strategy to insert a spiked tool into soil with a compliant light weight robot. Our method is based on Cartesian impedance control with an additional feed-forward force term, as described in Sec. 3. This term is calculated w. r. t. the soil properties based on three methods, namely the Fundamental Earth-Moving Equation and the Discrete Element Method and an empirical method. We compare our approach with a state-space control strategy, and Cartesian impedance control *without* feed-forward force term in a set of elaborate experiments in Sec. 4. We evaluate our approach with three different soil samples, possibly found in extraterrestrial environments.

2. RELATED WORK

Robot interaction with the environment has been a constantly expanding area of research. Constrained robot movement poses some very challenging tasks mainly concerned with maintaining stability in cases of transition from unconstrained to constrained motion, unknown environments or environments with variable properties. This problem becomes all the more difficult if the robot interacts with the environment while using a tool, such as a geophone, to be inserted into soil with possibly unknown properties. This problem can be solved using either hybrid force/position control or *impedance control*. The concept of impedance control was first proposed by Hogan [5] and was motivated by the fact that separate control of position and force is not sufficient in case of dynamical interaction between a manipulator and the environment. The *operational space formulation* by Khatib [6] enabled control formulation in the task space instead of in the joint space. This led to the introduction of *Cartesian impedance controllers*, as described by Ott [7]. In [8], a modified controller for work in environments with unknown properties is proposed by introducing an estimated feed-forward force term.

Analysis of soil-tool interaction is a very wide research area in geophysics, but little work was done in combining this work with robotic manipulation for the purpose of process automation. Basics of soil mechanics for cohesionless and cohesive soils are presented in [9]. In [10], Reece argues that all soil forces can be described by a single equation. He studied a problem of blade cutting into the soil and proposes a *Fundamental Earth-Moving Equation (FEME)*. This equation has become a starting point for many soil-tool interaction analysis. An advanced modification of Reece's fundamental equation was developed by Chung and Sudduth [11] w. r. t. a cone penetrometer, traveling vertically through soil.

Nowadays, there are many software tools for simulating soil behavior and computing force as a result of soil-tool interaction. Most work in this area is based on the *Discrete Element Method (DEM)* developed by Cundall and Struck [12]. The open-source software *YADE-DEM* implements the Discrete Element Method [13] for the simulation of granular materials. It is frequently used for the analysis of physical parameters of the soil and often in the analysis of soil-tool interaction. Obermeyer *et al.* predict horizontal draft forces for a thin metal plate moving through cohesionless soil, using YADE-DEM [14]. Modenese *et al.* analyzed lunar soil behavior using DEM modeling in YADE-DEM [15]. The conclusion was made that lunar soil shows unusual cohesion in comparison to the terrestrial soil of the same mineralogy. That is explained by higher surface energies resulting from different environmental conditions, i. e. low gravitational acceleration, very low pressure, and very high temperatures. Therefore, higher forces need to be exerted in order to break the soil while inserting a tool.

The closest related research to our work can be found in the field of automated excavation and digging processes. In [16], Luengo *et al.* suggest to model closed loop behavior based on predicted soil resistance forces. Robot-soil interaction was studied by Hong [17]. The author presented different soil models and different robot control methodologies, implemented for the purpose of obtaining soil parameters from the interaction of robot manipulator with the soil. In [18], ground coupling of a spiked geophone with the ground was studied. The geophone was considered as a cylinder and it was shown that ground coupling is dependent on the length of spike.

3. AUTOMATED GEOPHONE DEPLOYMENT

Inserting a spiked geophone sensor into soil is a challenging task for a robot since the soil parameters are variable and difficult to estimate. Therefore, we investigate the problem of soil-tool interaction w. r. t. both the geological aspects of the problem as well as the aspects of the robotic control system. This is done by using a Cartesian impedance controller with a feed-forward force term outlined in Sec. 3.1. The feed-forward force component of the controller is estimated with two traditional methods dealing with tool-soil interaction, namely the *Fundamental Earth-Moving Equation (FEME)* and the *Discrete Element Method (DEM)*. The FEME method is a simplified analytical approach to desribe continuous tool-soil interaction according to the mathematical model of a blade inserted into soil. This method can be applied to cohesionless and cohesive soil which enables the simulation of fine-grained, cohesive lunar regolith, which is outlined in Sec. 3.2. On the contrary the simulation based DEM method is able to simulate larger, irregular particles and resulting discontinuities such as the medium-sized, light lunar basalt rocks. This method is detailed in Sec. 3.3. Additionally, a third empirical method is proposed to describe the soil resistance force if the soil parameters are unknown in Sec. 3.4. The robot itself is thereby utilized to explore the soil properties by inserting the geophone with a stiff position control strategy to measure the external forces.

3.1. Cartesian Impedance Control with Feed-Forward Force Term

Impedance control enables simultaneous control of force and motion by defining a virtual, spatial impedance between the current and the desired robot configuration. Therefore, it is applicable for constrained tasks as it limits environmental force via the constant relation between force and motion. The impedance control action in the Cartesian space for the regulation task and with the assumption of a quasi-static task execution, i.e. $\ddot{\boldsymbol{x}} \approx \mathbf{0}$, can be defined as following:

$$\boldsymbol{f}_c = -\boldsymbol{D}_x\dot{\boldsymbol{x}} - \boldsymbol{K}_x(\boldsymbol{x} - \boldsymbol{x}_d) \tag{1}$$

where the vector $\boldsymbol{f}_c \in \mathbb{R}^6$ is the wrench exerted by the robot, $\boldsymbol{D}_x \in \mathbb{R}^{6x6}$ is the virtual damping matrix of the manipulator in the Cartesian space and $\boldsymbol{K}_x \in \mathbb{R}^{6x6}$ the virtual stiffness matrix of the robotic manipulator in the Cartesian space. A desired robot configuration is denoted as $\boldsymbol{x}_d \in \mathbb{R}^6$, while a current robot configuration is denoted as $\boldsymbol{x} \in \mathbb{R}^6$. Accordingly, $\dot{\boldsymbol{x}} \in \mathbb{R}^6$ is a current robot velocity. The virtual damping matrix, $\boldsymbol{D}_x$, is computed using the double diagonalization approach [19]. The rotational component of the impedance equation is based on quaternions [20]. At this stage, only a decoupled behavior is considered, i.e. the matrices $\boldsymbol{D}_x$ and $\boldsymbol{K}_x$ are diagonal. In the task of inserting a spiked geophone, precise positioning and good coupling with the soil are mandatory. The Cartesian impedance control should be extended w. r. t. to these requirements to allow for an explicit bound on the interaction force. Therefore, we propose a *feed-forward force term* to overcome the soil resistance force. The dynamical equation of the robotic system in the Cartesian space, with the included feed-forward force term, is described as follows:

$$\boldsymbol{M}(\boldsymbol{x})\ddot{\boldsymbol{x}} + \boldsymbol{C}(\boldsymbol{x}, \dot{\boldsymbol{x}})\dot{\boldsymbol{x}} + \boldsymbol{g}(\boldsymbol{x}) = \boldsymbol{f}_c + \boldsymbol{f}_d + \boldsymbol{f}_e \tag{2}$$

where the components $\boldsymbol{M}(x) \in \mathbb{R}^{6x6}$, $\boldsymbol{C}(\boldsymbol{x}, \dot{\boldsymbol{x}}) \in \mathbb{R}^{6x6}$ and $\boldsymbol{g}(\boldsymbol{x}) \in \mathbb{R}^6$ represent the inertial matrix, the matrix of Coriolis and centrifugal contributions to the force and the gravitation vector of the robotic system in the Cartesian space, respectively. Furthermore, $\boldsymbol{f}_c \in \mathbb{R}^6$ is the control action of the Cartesian impedance controller (i. e. the wrench exerted by the robot on the environment), while the $\boldsymbol{f}_d \in \mathbb{R}^6$ is the feed-forward force term (i. e. the desired force exerted by the robot) and $\boldsymbol{f}_e \in \mathbb{R}^6$ is the vector of external wrenches exerted by the environment (soil). Please note that the vertical motion of geophone insertion is studied in this paper solely. Accordingly, only the vertical, translational component $f_{d,3}$ is of interest. Hence, in the remaining paper only the force component $f_{d,3}$ (and analogously $f_{e,3}$) will be considered.

In order to predict $f_{d,3}$, detailed knowledge of the interacting environment is required. In case of the task of geophone insertion, the prediction of the interaction force between the soil and the spike depends mainly on the soil properties. Three prediction methods are described in the following sub-sections.

3.2. Fundamental Earth-Moving Equation

One way to predict the soil resistance force is the so-called *Fundamental Earth-Moving Equation (FEME)* by Reece [10]. It describes a mathematical model in 2D, developed to theorize the design of machines used for moving soil, e. g. in excavation or digging applications. The author developed the equation based on the example of a blade cutting into soil with low velocity until complete soil failure. A resistance force exhibited between the soil and the moving tool can generally be represented as follows:

$$F = f(\gamma, q, c, c_a, \phi, \delta, d, \alpha, \theta), \tag{3}$$

where F is a scalar of the total resistance force magnitude of the soil, acting on the tool during its insertion, γ is the unit weight of the soil, q represents any additional surcharge effects, c is the cohesion of the soil, c_a is the adhesion between the soil and the tool, ϕ is the internal friction angle of the soil, δ is the friction angle between the soil and the tool, d is the depth to which the tool has been inserted into the soil, and α is the angle of the tool inclination when inserted into the soil. θ has to be defined w. r. t. the geometric properties arising from the shape of the tool, such as the diameter of a geophone spike w_t.

In a nutshell, the resistance force of the soil acting on the tool depends on the *soil properties* (density, internal angle of friction, cohesion) and the *tool properties* (width, length, angle of inclination). The FEME equation, proposed by Reece, is adapted in this paper by assuming a triangular failing surface instead of a logarithmic one, as we operate in shallow depths. Since only low velocities of insertion are considered, the damping contribution to the reaction force of the soil during the insertion can be neglected. In this case, the intensity of the reaction force exerted on the tool by the soil can be calculated as follows:

$$F = \gamma d^2 w_t N_\gamma + q d w_t N_q + c d w_t N_c + c_a d w_t N_a \tag{4}$$

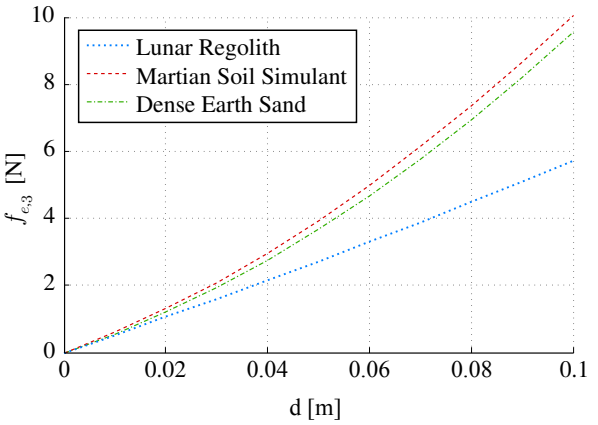

Figure 2. The FEME Method applied to three exemplary soil samples. Note that the lunar regolith (blue, dotted), was computed w. r. t. lunar gravitational conditions, where $g = 1.62519\,m\,/\,s^2$

The four main terms in (4) represent the effects of the *weight* of the soil, any *surcharge*, the *cohesion*, and the *adhesion* between the soil and the tool. The N factors are dimensionless numbers describing the shape of the *soil failure surface*. Based on (4), the intensity of the vertical force is obtained by a vector decompositon:

$$f_{e,3} = F * cos(\alpha + \delta) \tag{5}$$

It is important to make a difference between *cohesionless* and *cohesive* soils at this point, since these properties affect resistive forces to the greatest extent. Cohesionless soil, e. g. dry sand, shows no bond between particles. On the contrary, cohesive soil, e. g. clay, shows high bond between the particles.

This analytical method can be utilized to predict the soil resistance force of cohesive, small to medium grain soil with varying properties as illustrated in Fig. 2. It is suitable to simulate the conditions of lunar regolith (simulant) and Martian soil (simulant), which constitutes soil sample number three in our experiment suite.

3.3. Discrete Element Method

One approach to predict the interaction forces for more complex scenarios, is the simulation based *Discrete Element Method (DEM)*. Unlike the Fundamental Earth-Moving Equation, DEM is a three dimensional approach which can be applied to more realistic tool shapes since it does not require any assumption of the soil failure surface shape. It is therefore often used to simulate wheel-soil interaction for extraterrestrial rovers [21]. Particles of a granular material, such as sand or gravel, are usually simulated as a set of spheres. To simulate more complex soil structures, several spheres can be combined to approximate *poly-ellipsoidal* particles. The tool interacting with the soil is defined as a set of vertices forming a rigid body. As a result, the method is able to compute interaction forces between the soil particles, and reaction forces

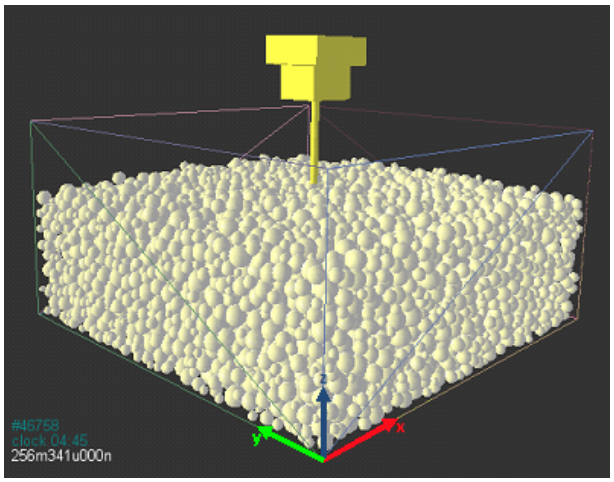

Figure 3. The simulated DEM tool-soil interaction computed and visualized with YADE-DEM for gravel.

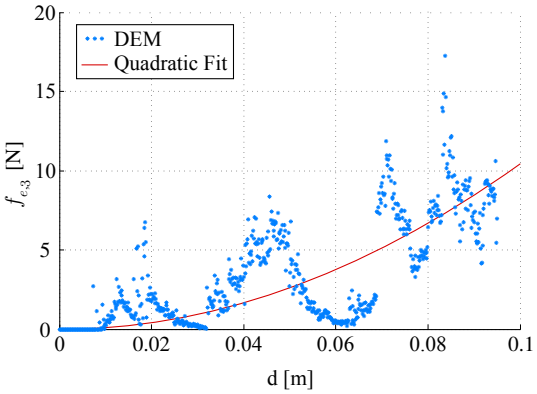

Figure 4. The predicted soil resistance force for gravel simulated with YADE-DEM.

between the soil and the tool. The discretized method is especially suitable to predict discontinuities resulting from soil which consists of larger particles, such as gravel or lunar basalt rocks. Simulating lunar regolith with the DEM approach is only applicable to a certain extent (with very small simulation steps), since the lunar regolith particles are very small compared to the surface of the geophone spike.

We use the open-source software *YADE-DEM* [13] to simulate the insertion of geophones into big grained soil, e. g. gravel or basalt rocks, as illustrated in Fig. 3. The simulation results unveil the discontinuities in the force profile. The spike moving with a constant velocity pushes the spheres until they move aside. That causes a free space in front of the spike allowing it to *fall through* that part of the soil almost undisturbed by the particles. This behavior is not recorded for soils with smaller particles, e. g. in the case of sands this effect is completely mitigated. A quadratic interpolation of the data can be used to approximate the feed-forward force of the impedance controller. This method is suitable to simulate lunar basalt rocks, which constitutes soil sample number one in our experiment suite.

3.4. Empirical Soil Parameter Prediction

Soil parameters are hard to predict in general. However, they are required to calculate the resistance force with the FEME and the DEM method. To overcome this issue, we propose an additional method to empirically relate the soil resistance force to a variable stiffness behavior. This is done by inserting the geophone with the robot with varying velocities by utilizing a position controller that is assumed to react infinitely stiff. The stiffness of the geophone spike is also assumed to be infinitely stiff and therefore negligible. Fig.5 shows an equivalent mechanical structure of the task set-up in the Cartesian space, where the end-effector, the geophone and the ground are represented by mechanical elements. The end-effector is replaced by a mass-damper-spring system, the geophone

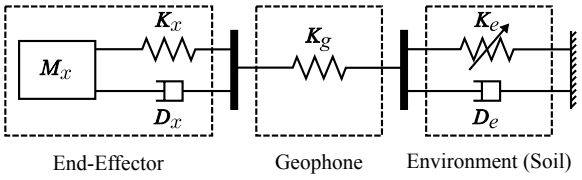

Figure 5. Equivalent representation of the end-effector, geophone and soil using mathematical elements mass, damper and spring.

by a spring only and the soil is considered as a visco-elastic material, represented by a damping and a variable stiffness. Note that the effect of the soil damping is neglected as only low velocities are considered. The mass of the soil is neglected as its quasi-static behavior is assumed.

The vertical component of the environment force is measured during the empirical estimation procedure with the position controller and can be related to the FEME equation as $f_{e,3} = Fcos(\alpha + \delta)$, if and only if $d > 0$. The FEME equation is a nonlinear function of the insertion depth d. All remaining parameters are constant for the proposed task. Consequently, it is possible to represent the FEME equation as a force-to-displacement equation where the force is related to displacement via a variable stiffness:

$$\begin{aligned} f_{e,3} &= \underbrace{\gamma w_t N_\gamma cos(\alpha+\delta)}_{C_1} d^2 + \\ &\underbrace{(q w_t N_q + c w_t N_c + c_a w_t N_a) cos(\alpha+\delta)}_{C_2} d \\ &= C_1(x_{e,3} - x_3)^2 + C_2(x_{e,3} - x_3) \\ &= K_e(x_3)(x_{e,3} - x_3) \end{aligned} \tag{6}$$

where $d = x_{e,3} - x_3$ with $x_{e,3}$ being the vertical location of the soil surface and x_3 being the vertical location of the geophone spike tip. The soil stiffness is: $K_e(x_3) = C_1(x_{e,3} - x_3) + C_2$, where C_1 and C_2 are constant parameters of the soil variable stiffness. This allows for an estimation of the constants C_1 and C_2 offline using the least-squares method. Analogously to (6), the desired force exerted by the robot in the vertical, translational direction, in the constrained and unconstrained subspace, can be defined as follows:

$$f_{d,3} = \begin{cases} K_e(x_{d,3})(x_{e,3} - x_{d,3}), & x_{d,3} \leq x_{e,3} \\ 0, & x_{d,3} > x_{e,3} \end{cases} \tag{7}$$

where $x_{d,3}$ is a translational, vertical component of a desired end-effector motion and $K_e(x_{d,3}) = C_1(x_{e,3} - x_{d,3}) + C_2$. In general, a well estimated feed-forward force compensates for the soil reaction force, while the impedance control action mitigates the effect of model uncertainties and external disturbances.

4. EXPERIMENTAL EVALUATION

We conduct a suite of experiments to evaluate the proposed Cartesian impedance control strategy with the mobile humanoid robot *Rollin' Justin* [22] of the *German Aerospace Center (DLR)*. It is equipped with a sensorized head, two *DLR LWR III light weight arms* and the *DLR HAND II* as end-effector. This robot is representative for the LRU rover [4] currently under development for the upcoming field mission of the ROBEX project. The experimental setup includes a geophone dummy, consisting of an *inertial measurement unit (IMU)* in a custom housing mounted on a cylindrical metal spike (90 mm long and 8 mm diameter), and three boxes filled with different soil samples: Big grained basalt rocks (22 - 8 mm), medium grain clay particles (8 - 2 mm), and small grain cohesive Martian soil simulant (< 2 mm). For each soil sample the force profile can be predicted with the prediction methods described in Sec. 3.2 and Sec. 3.3 if the soil parameters are available. In particular, the big grained basalt rocks are best simulated with YADE-DEM, and the FEME method is applicable to the two smaller grains. If the soil parameters are unknown, the empirical method described in Sec. 3.4 can be utilized to predict the soil stiffness offline with the least-squares approach. The parameters given in Table 1 represent the average values of the identified parameters.

For each soil sample, the robot has to insert the geophone dummy by utilizing three different control strategies: State-space control, Cartesian impedance control, and Cartesian impedance control with feed-forward force term according to the predicted soil resistant force. For each trial the robot is commanded to grasp the geophone and hold it above the sample container. In this position, the IMU data of the geophone dummy is used to estimate the geophone orientation and to realign it w. r. t. the surface normal of the soil below. Afterwards, the geophone spike is placed on top of the soil, not yet penetrating it, to mark the starting position for the trial. The geophone is inserted by executing a vertical straight line trajectory until the spike is fully inserted into the soil layer to ensure good coupling and no tilting (see Fig. 1). Note that not all soil samples have the same fill level, which results in different penetration depths. Before each trial, the soil is mechanically loosened to ensure a similar ground compaction. During the insertion procedure, the desired and measured Cartesian position (see Fig. 6), as well as the soil reaction forces are recorded (see Fig. 7). The experiments where executed with an average desired Cartesian velocity of 38 mm/s.

Soil Sample	C_1	C_2
Basalt Rocks	232.0	12.3
Clay Particles	444.5	23.9
Martian Soil Simulant	269.9	9.7

Table 1. Average stiffness parameters of the soil samples.

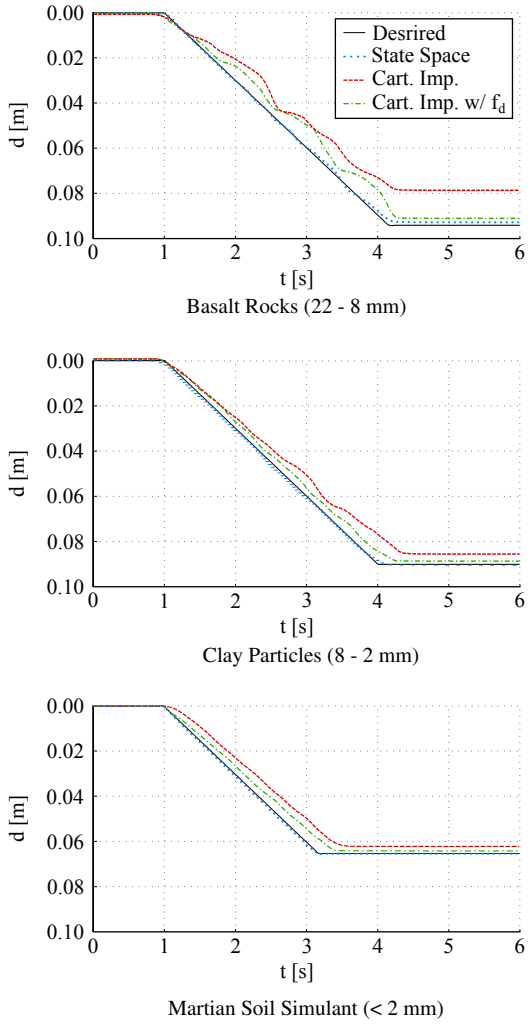

Figure 6. The desired penetration depth (black, solid) compared to the measured trajectories executed with different control strategies, namely state-space control (blue, dotted), Cartesian impedance control (red, dashed), and Cartesian impedance control with feed-forward force term (green, chain-dotted).

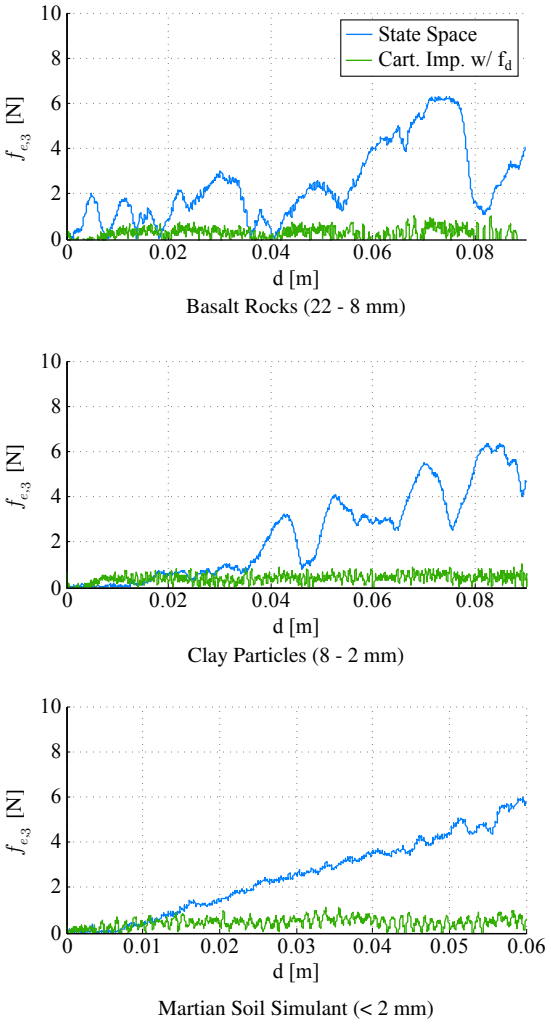

Figure 7. Comparison of the soil reaction forces observed while inserting the geophone with the state-space controller (blue) and the Cartesian impedance controller with feed-forward force term (green).

A displacement plot for all control strategies and all soil samples is shown in Fig. 6. In general the state-space controller performs well in the tracking task (low tracking error) as well as in the regulation task (low steady-state error, < 1 mm) for all types of soil. The default Cartesian impedance controller shows the highest steady-state error for all types of soil (up to 15 mm for the basalt rocks). By including the soil model, the Cartesian impedance controller with feed-forward force term performs comparable to the state-space controller in terms of tracking error and steady-state error (< 3 mm) for all types of soil. The state-space controller is stiff in all Cartesian dimensions. In contrary both impedance control strategies act compliant in the direction of motion, as well as in the other dimensions. This way the robot is able to adapt the motion w. r. t. unknown obstacles, such as larger rocks in the ground. This behavior can be observed in the displacement plot for the basalt rocks. As the coupling between the geophone and the ground is best when it is entirely inserted [18], the Cartesian impedance controller without feed-forward force term is not suited for the task of geophone insertion.

The soil reaction force is illustrated in Fig. 7 for the state-space controller and the Cartesian impedance controller with feed-forward force term. The state-space controller increases the force to penetrate the soil with the geophone. The resulting force plot for the first sample container filled with basalt rocks is comparable to the simulated scenario of gravel in YADE-DEM illustrated in Fig. 4. The force oscillates between zero and relative high values all the way through the soil, starting already at the soil surface. A similar, but more moderate oscillation can be observed for the medium sized clay particles. The oscillation for the small grained Martian soil simulant is negligible, however, the force increases constantly.

In comparison the Cartesian impedance controller with feed-forward force term limits the soil reaction force. It is always close to zero in the direction of motion.

We have observed tilting of the geophone after it was released by the robot when using either of the two control strategies. Both strategies failed in some trials, as they exceeded the maximum allowed tilting angle of 7° [1]. In average, the Cartesian impedance controller with feed-forward force term showed improved coupling between the geophone spike and the ground. Consequently the geophone tilted less in most of the trials. However, we could not generate reproducible measurements as severe tilting was randomly introduced by the adhesion between the rubber of the fingers and the housing of the geophone when releasing it. This effect will be compensated by a dedicated docking interface design, which is currently under development for the upcoming ROBEX field mission.

5. DISCUSSION

In this work we have shown that a light weight robot is able to precisely deploy a seismic sensor in various types of soil. We utilize Cartesian impedance control with a feed-forward force term to ensure precise positioning and good coupling. The feed-forward force term is designed to overcome the soil resistance force which can be predicted, analytically with the FEME approach, numerically with the DEM approach, or empirically by exploring the soil properties with the robot in advance. The proposed control strategy reduces the tilting of the geophone as it is required by the seismic network to guarantee accurate geological experiments.

Different types of soil and different tools, i. e. seismometers, may require different deployment strategies. Especially lunar conditions may lead to different requirements for the deployment. Therefore, the insertion strategies are integrated in so-called *Action Templates* which provide a flexible way to develop process models for arbitrary manipulation tasks [23]. The object-centered approach of Action Templates make them robot independent per definition. They can be utilized by the LRU rover in the upcoming field mission without adaption. This rover will be equipped with a docking interface instead of a robotic hand to further reduce the positioning and tilting error. As a result, the robotic deployment of seismic networks can be executed more accurate, more reliable, and without endangering astronauts. As conclusion we encourage to consider automated seismic sensor deployment for future extraterrestrial exploration missions.

ACKNOWLEDGMENTS

This work was supported by the Helmholtz Association, project alliance ROBEX, under contract number HA-304.

The authors would like to thank Alexandra Czeluschke of the DLR Institute of Planetary Research for the discussions about her ongoing research on the re-evaluation of the Apollo 17 Lunar Seismic Profiling Experiment based on new recordings captured with the Lunar Reconnaissance Orbiter Camera.

REFERENCES

[1] T. Sullivan, "Catalog of apollo experiment operations," *NASA Reference Publication*, no. 1317, 1994.

[2] A. Czeluschke, M. Knapmeyer, J. Oberst, and I. Haase, "New lunar depth profiles derived from lroc-based coordinates of apollo 17 seismic equipment," in *In Proc. of the European Lunar Symposium*, May 2015.

[3] A. Wedler, C. Waldmann, G. Meinecke, M. Wilde, L. Witte, C. Lange, N. Schmitz, M. Knapmeyer, O. Pfannkuche, L. Thomsen, S. Flgel, R. Rosta, T. Bellmann, M. Hellerer, B. Rebele, H. Gmeiner, B. Vodermayer, and Y. Takei, "ROBEX - components and methods for the planetary exploration demonstrationmission," in *Proc. of the 13th Symposium on Advanced Space Technologies in Robotics and Automation (ASTRA)*, May 2015.

[4] A. Wedler, B. Rebele, J. Reill, M. Suppa, H. Hirschmller, C. Brand, M. Schuster, B. Vodermayer, H. Gmeiner, A. Maier, B. Willberg, K. Bussmann, F. Wappler, and M. Hellerer, "LRU - lightweight rover unit," in *Proc. of the 13th Symposium on Advanced Space Technologies in Robotics and Automation (ASTRA)*, May 2015.

[5] N. Hogan, "Impedance control: An approach to manipulation," *ASME Journal of Dynamic Systems, Measurement and Control*, vol. 107, pp. 17–24, June 1985.

[6] O. Khatib, "A unified approach for motion and force control of robot manipulators: The operational space formulation," *IEEE Journal on Robotics and Automation*, vol. RA-3, pp. 43–53, February 1987.

[7] C. Ott, *Cartesian Impedance Control of Redundant and Flexible-Joint Robots*, vol. 49 of *Springer Tracts in Advanced Robotics*. Springer Publishing Company, Berlin Heidelberg, 2008.

[8] C. Yang, G. Ganesh, S. Haddadin, S. Parusel, A. Albu-Scheffer, and E. Burdet, "Human-like adaptation of force and impedance in stable and unstable interactions," *IEEE Transactions on Robotics*, vol. 27, pp. 918–930, October 2011.

[9] K. Terzaghi, *Theoretical Soil Mechanics*. New York: John Wiley and Sons, 1943.

[10] A. Reece, "The fundamental equation of earth-moving mechanics," *Proceedings of the Institution of Mechanical Engineers*, vol. 179, pp. 16–22, June 1964.

[11] S. Chung and K. Sudduth, "Soil failure models for vertically operating and horizontally operating strength sensors," *American Society of Agricultural and Biological Engineers*, vol. 49, no. 4, pp. 851–863, 2006.

[12] P. Cundall and O. Strack, "A discrete numerical model for granular assemblies," *Geotechnique*, vol. 29, pp. 47–65, 1979.

[13] J. Kozicki and F. Donzé, "A new open-source software developed for numerical simulations using discrete modeling methods," *Computer Methods in Applied Mechanics and Engineering*, vol. 197, no. 49, pp. 4429–4443, 2008.

[14] M. Obermayr, K. Dressler, C. Vrettos, and P. Eberhard, "Prediction of draft forces in cohesionless soil with the discrete element method," *Elsevier Journal of Terramechanics*, vol. 48, pp. 347–358, September 2011.

[15] C. Modenese, S. Utili, and G. Houlsby, "DEM modelling of elastic adhesive particles with application to lunar soil," in *Proc. of the Earth and Space 2012 Conference*, pp. 45–54, April 2012.

[16] O. Luengo, S. Singh, and H. Cannon, "Modeling and identification of soil-tool interaction in automated excavation," in *Proc. of the IEEE/RSJ International Conference on Intelligent Robots and Systems*, pp. 1900–1906, 1998.

[17] W. Hong, *Modeling, Estimation and Control of Robot-Soil Interactions*. PhD thesis, Massachusetts Institute of Technology, September 2001.

[18] G. Drijkoningen, F. Rademakers, E. Slob, and J. Fokkema, "A new elastic model for ground coupling of geophones with spikes," *Geophysics*, vol. 71, pp. Q9–Q17, March-April 2006.

[19] A. Albu-Schffer, C. Ott, and G. Hirzinger, "A passivity based cartesian impedance controller for flexible joint robots - part ii: Full state feedback, impedance design and experiment," in *Proc. of the IEEE International Conference on Robotics and Automation (ICRA)*, vol. 3, pp. 2666–2672, April 2004.

[20] F. Caccavale, C. Natale, B. Siciliano, and L. Villani, "Six-dof impedance control based on angle/axis representations," *IEEE Transactions on Robotics and Automation*, vol. 2, pp. 289–300, April 1999.

[21] M. A. Knuth, J. Johnson, M. Hopkins, R. Sullivan, and J. Moore, "Discrete element modeling of a mars exploration rover wheel in granular material," *Journal of Terramechanics*, vol. 49, no. 1, pp. 27–36, 2012.

[22] C. Borst, T. Wimböck, F. Schmidt, M. Fuchs, B. Brunner, F. Zacharias, P. R. Giordano, R. Konietschke, W. Sepp, S. Fuchs, *et al.*, "Rollin'justin-mobile platform with variable base," in *Proc. of the IEEE International Conference on Robotics and Automation (ICRA)*, pp. 1597–1598, 2009.

[23] D. Leidner, C. Borst, and G. Hirzinger, "Things are made for what they are: Solving manipulation tasks by using functional object classes," in *Proc. of the IEEE/RAS International Conference on Humanoid Robots (ICHR)*, pp. 429–435, 2012.